Fracture Mechanics of Concrete and Concrete Structures - Recent Advances in Fracture Mechanics of Concrete - B. H. Oh, et al.(eds)

Application of an anisotropic damage model to the prediction of early age cracking.

L. Buffo-Lacarrière & A. Sellier
Université de Toulouse; UPS, INSA; LMDC 135, avenue de Rangueil; 31 077 Toulouse Cedex 04; France

ABSTRACT: The purpose of this work was the design and validation of a simulation toolbox able to predict the early age cracking of concrete structures in order to help in the choice of adequate technical solutions. The numerical toolbox was developed in the finite element code CASTEM and is based on an anisotropic damage model associated with a rheological and a hydration model in order to assess the risk of cracking of reinforced structures at early age. The work presented was done in the framework of the national project CEOS.fr, which is intended to test and improve the modeling of the cracking of reinforced concrete structures and more especially in the research area that deals with thermal and drying-induced cracking (THM behavior).

1 INTRODUCTION

The early age cracking of structures is a serious preoccupation in the construction industry. The occurrence of cracks in structures during the construction phase is not acceptable and is considered as a construction failure. In this context, the purpose of the work presented here was to develop a numerical simulation tool able to quantify the early age cracking risk of in situ structures in order to help in the choice of appropriate concrete formulations and construction techniques to prevent or limit this risk.

The numerical tool proposed in this paper is based on an anisotropic damage model associated with a rheological model and a hydration model in order to assess the risk of cracking of reinforced structures at early age. The multiphasic hydration model predicts the evolution of hydration degree and temperature, which is used in the rheological model to evaluate the induced stresses. The necessity to use a rheological model instead of an elastic one as proposed in several codes (CESAR LCPC, 4C-Temp&Stress) has been demonstrated in (Benboudjema & Torrenti 2008). The other originality of the proposed model is the anisotropy of the damage model and its adaptation to the behavior of hardening concrete.

The paper first presents the anisotropic damage model and its validation by a monotone test performed on hardened concrete. Then it develops the adaptation needed for an application to hardening concrete that is subjected to physicochemical variations. This model for hardening concrete is finally applied to a massive wall that experimentally revealed early age cracking.

2 MECHANICAL MODEL FOR HARDENED CONCRETE

2.1 *Anisotropic damage model*

The model is based on the well known effective stress concept proposed by Kachanov (1986), in which the effective stresses are assessed using the equivalent strain principle. According to this principle, the effective stress tensor, which represents the stress in the undamaged zone of a representative elementary volume, can be assessed using the elastic constants of the sound material:

$$\tilde{\boldsymbol{\sigma}} = k^0 .tr(\boldsymbol{\varepsilon}^e)\mathbf{I} + 2\mu^0(\boldsymbol{\varepsilon}^e - tr(\boldsymbol{\varepsilon}^e)\mathbf{I}) \quad (1)$$

where:
- $\tilde{\boldsymbol{\sigma}}$ is the tensor of effective stresses,
- $\boldsymbol{\varepsilon}^e$ is the tensor of the elastic strains,
- $\mathbf{I}$ is the second order identity tensor,
- k^0 and μ^0 are the bulk and shear moduli.

Once the effective stress tensor is known, the effects of the opening and re-closing of existing cracks on the material stiffness are treated through a spectral decomposition of the effective stress tensor, according to the sign of the main stress.

The spectral decomposition uses a classical diagonalization algorithm which supplies the main stresses and corresponding main directions:

$$\tilde{\boldsymbol{\sigma}} = \tilde{\sigma}_I \left(\vec{e}_I \otimes \vec{e}_I\right) \quad (2)$$

where $\vec{e}_I$ defines the main direction I.

The tensors of effective tensile and compressive stresses can be immediately deduced according to the sign of each main stress:

- if the main stress is a tension:

$$\tilde{\sigma}_I^t = \tilde{\sigma}_I \quad \text{and} \quad \tilde{\sigma}_I^c = 0 \tag{3}$$

- if the main stress is a compression:

$$\tilde{\sigma}_I^t = 0 \quad \text{and} \quad \tilde{\sigma}_I^c = \tilde{\sigma}_I \tag{4}$$

Once this decomposition is achieved, effective tensile stresses are modified by tensile damage and effective compressive stresses by compressive damage to obtain the apparent stresses.

For the compressive case, damage is isotropic (based on a Drucker-Prager criterion). Thus once a simple scalar damage variable is used, it affects compression effective stresses directly:

$$\boldsymbol{\sigma}^{\mathbf{c}} = (1 - d^c)\tilde{\boldsymbol{\sigma}}^{\mathbf{c}} \tag{3}$$

In tension, damage is model by a fourth order tensor applied to the tensile effective stresses:

$$\boldsymbol{\sigma}^{\mathbf{t}} = (\mathbf{I} - \mathbf{D}^{\mathbf{t}})\tilde{\boldsymbol{\sigma}}^{\mathbf{t}} \quad \Leftrightarrow \quad \sigma_{mn}^t = \left(\delta_{mn,op} - D_{mn,op}^t\right)\tilde{\sigma}_{op}^t \tag{6}$$

In the proposed model, the damage variable is evaluated from the cracking state of the material. This cracking state is represented as a second order tensor admitting the classical spectral decomposition in main values d_m^t:

$$\mathbf{d}^{\mathbf{t}} = d_m^t \left(\vec{e}_m \otimes \vec{e}_m\right) \tag{4}$$

where $\vec{e}_m$ is an eigenvector of the damage tensor.

The expression for the damage variable D according to this crack variable d is obtained by considering that the Young's modulus in each main direction of the tensile damage tensor is differently affected, which confers an orthotropic aspect on the model. The Poisson coefficient must also decrease in the same way as the corresponding Young's modulus. This last assumption causes the Poisson effect to vanish progressively in the two directions orthogonal to a tensile damage main direction, which leads to a progressive decoupling of the behavior in the different main directions when tensile damage increases. This is also a classical experimental observation that is widely adopted by practitioners, notably to compute reinforcements in cracked slabs.

The relationship between effective and apparent stresses in tension is thus proposed assuming that the strain equivalence principle is written successively between:

- apparent stresses and elastic strains (Equation (8)). This Equation is defined using the rigidity matrix of the damaged material R^D.

$$\begin{cases} \varepsilon_{mm}^e = \dfrac{\sigma_{ii}}{E^0(1-d_m^t)} - \dfrac{\upsilon^0}{E^0}\left(\sigma_{nn} + \sigma_{oo}\right) \\ \varepsilon_{mn}^e = \dfrac{\sigma_{mn}}{\mu^0(1-d_m^t)(1-d_n^t)} \end{cases} \tag{8}$$
$$\Leftrightarrow \varepsilon_{mn}{}^e = \left(R_{mn,op}{}^D\right)^{-1}\sigma_{op}$$

- effective stresses and elastic strains (Equation (9)). This Equation is defined using the rigidity matrix of the sound material R^0.

$$\begin{cases} \varepsilon_{mm}^e = \dfrac{\tilde{\sigma}^t{}_{mm}}{E^0} - \dfrac{\upsilon}{E^0}\left(\tilde{\sigma}^t{}_{nn} + \tilde{\sigma}^t{}_{oo}\right) \\ \varepsilon_{mn}^e = \dfrac{\tilde{\sigma}^t{}_{mn}}{\mu^0} \end{cases} \tag{5}$$
$$\Leftrightarrow \varepsilon_{mn}{}^e = \left(R_{mn,op}{}^0\right)^{-1}\tilde{\sigma}_{op}$$

Combining the last two sets of Equations leads to the definition of the fourth order damage tensor:

$$D^t{}_{mn,op} = \delta_{mn,op} - \left(R_{mn,rs}{}^0\right)^{-1}\left(R_{rs,op}{}^D\right)^{-1} \tag{10}$$

During cyclic loading, if a crack has been created in direct tension, its effect on the stiffness matrix is modeled according to the last Equation. Its reclosure when the stress sign changes is treated by considering compressive instead of a tensile damage as soon as the corresponding effective stress becomes a compression one. In contrast, if the concrete has been first damaged in compression, it is impossible to re-close all the micro-cracks induced by the crushing phenomena, so when the effective stress becomes a tensile one, the effect of the compression damage must be kept even in tension. To model this dissymmetry properly in the unilateral behavior of concrete, it is necessary to adopt the final following formulation:

$$\boldsymbol{\sigma} = (1 - D^c).(\tilde{\boldsymbol{\sigma}}^{\mathbf{c}} + (\mathbf{I} - \mathbf{D}^{\mathbf{t}})\tilde{\boldsymbol{\sigma}}^{\mathbf{t}}) \tag{11}$$

The evolution law for the damage is inspired by the Weibull law (Sellier & Bary 2002) classically used to describe the effects of defects in brittle materials (Equation (12)) and leads to a behavior law of the form presented in Figure 1. Note in the Equations (12) that as the crack variable d_m is expressed

according to the effective stresses (through the threshold stress), the damage model does not need under-iteration on the time step (as plastic damage models).

$$d_m^t = 1 - \exp\left(-\frac{1}{p^t} \left(\frac{\overline{\sigma}_i^t}{\widetilde{\sigma}_u^t} \right)^{p^t} \right)$$

$$d^c = 1 - \exp\left(-\frac{1}{p^c} \left(\frac{\overline{\sigma}^c}{\widetilde{\sigma}_u^c} \right)^{p^c} \right) \quad (12)$$

where: - $\overline{\sigma}$ is the equivalent threshold stress that characterizes the material stress history. It is evaluated with failure criteria according to the sign of the main stresses. For tensile damage, the Rankine criterion is used (in each direction i), while for compressive damage, the threshold stress is determined using the Drucker-Pragger criterion, expressed with the effective stresses.

- p and $\widetilde{\sigma}_u$ are material parameters linked to the strength and the strain reached at the peak of the behavior law.

The localization problem induced by the softening behavior of concrete (Figure 1) is managed using a method inspired by Hillerborg et al. (1976), which modifies the post-peak part of the behavior law in order to control dissipation.

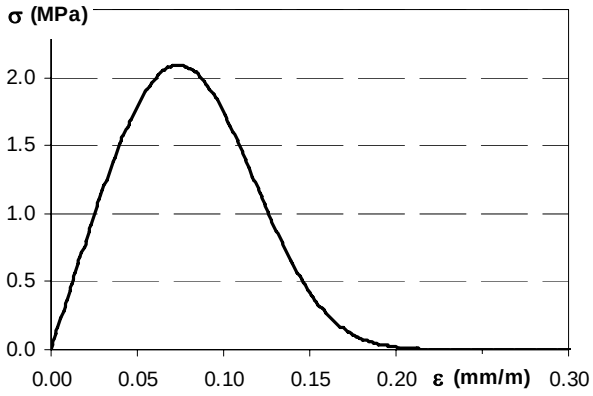

Figure 1. Tensile behavior law.

2.2 *Validation of the mechanical model on hardened concrete*

The proposed model was tested according to the prediction of a bending test performed up to the failure of the concrete beam. Figure 2 presents the damage field obtained with the proposed damage model before the failure. Note that the anisotropic damage model gives a good reproduction of the crack mapping classically obtained for this test.

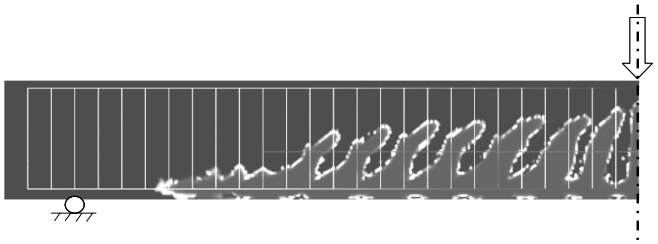

Figure 2. Damage field on the half beam.

Figure 3 shows the bending behavior law obtained with the model throughout the test. It especially shows the crack development during the test and the fact that the model successfully reproduces the rotation of the crack direction at the end of the test.

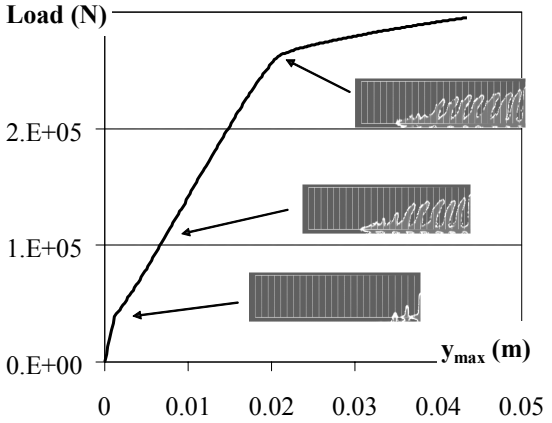

Figure 3. Bending behavior law obtained with the model.

3 VARIATIONS IN CONCRETE AT EARLY AGE

3.1 *Physicochemical variations*

In the framework of the early age behavior of a massive structure, the physicochemical variations that will have an impact on the mechanical behavior of the structure are the hydration degree and the temperature. On the one hand, the development of hydration in concrete leads to an increase in the mechanical properties as soon as the hydration degree reaches a critical value defined as the percolation threshold (see section 3.2). On the other hand, the variation of temperature leads to an internal thermal strain that can cause stress in the structure even without external loading (see section 3.3).

These physicochemical variations are predicted using the multiphasic hydration model proposed in (Buffo-Lacarrière et al. 2007). For an application to a massive structure, it combines the heat balance Equation with several kinetic hydration laws: one for each anhydrous composing the binder (clinker and pozzolanic additions) (Equation (13)).

$$\begin{cases} \rho c \dfrac{\partial T}{\partial t} = div(k \cdot \overrightarrow{grad\, T}) + \sum_i f_i Q_i^{th} \dot{\alpha}_i \\ \dot{\alpha}_i = f(\alpha, T, W, CH) \end{cases} \quad (13)$$

where: - k is the concrete conductivity,
- T is the temperature,
- α is the hydration degree
- W is the water content,
- CH is the content of calcium hydroxide,
- subscript i is relative to the anhydrous i (clinker or pozzolanic additions).

3.2 *Induced variation of the mechanical properties*

A variation law (Eq. (14) and Figure 4) for hardening concrete is proposed to reproduce the increase in mechanical properties (Pi) when the hydration degree reaches the mechanical percolation threshold. This percolation threshold is usually the same for all the mechanical properties. The proposed law is inspired by De Schutter (2002) and the calibration procedure for this variation law (based on mechanical tests performed at several ages) is presented in (Buffo-Lacarriere 2007).

$$P^i = P_\infty^{\ i} \cdot G^i(\alpha - \alpha_s) \quad (14)$$

where: - P_∞ represents the characteristic of totally hydrated concrete,
- α_s is the mechanical percolation threshold, taken as 0.15 for concrete (Byfors 1980, Torrenti & Benboudjema 2005).

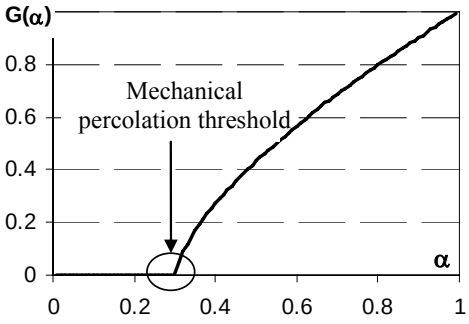

Figure 4. Evolution of variation law according to hydration.

3.3 *Stress induced by thermal strain*

In the framework of a massive structure at early age (no external loading), a creep model must be used to determined the effective stresses induced by the internal thermal strain ($\beta \cdot \dot{T}$), which is needed in the damage model to evaluate the risk of cracking.

The proposed creep model is inspired by the physical observations of Acker & Ulm (2001). The stress is split into spherical (superscript (s) in Figure 5) and deviatoric (superscript (d)) parts in order to reproduce the different creep behavior under these two kinds of load. The rheological behavior of the concrete is modeled by a system including an elastic level (0 in Equation (15)), for instantaneous behavior, and two creep levels (Figure 5).

The first creep module is a Kelvin-Voigt viscoelastic module, which reproduces the reversible creep (KV in Equation (15)), and the second is a Maxwell module with a non-linear viscosity, which models the irreversible creep (M in Equation (15)). The latter constitutes the originality of the proposed model.

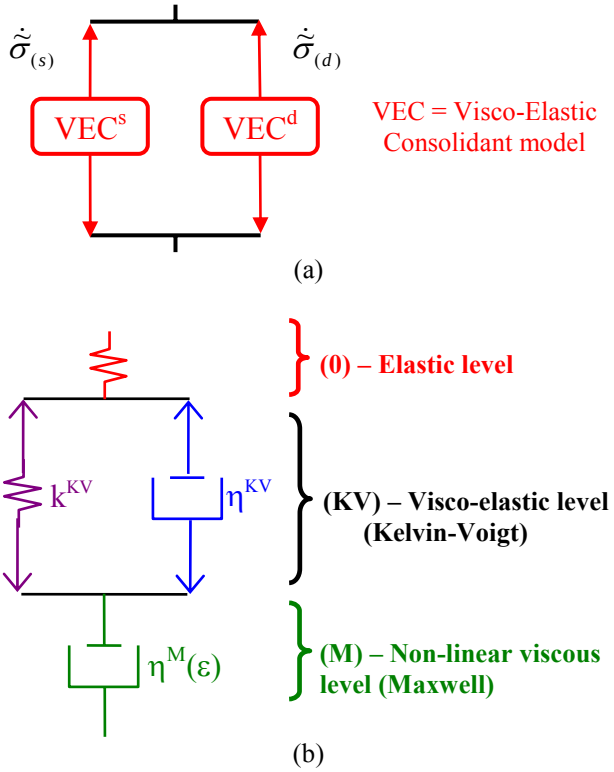

Figure 5. Illustration of stress splitting (a) and rheological scheme for VEC module (b).

The model is mathematically expressed by the system of Equations (15) for the spherical part of the stress (for the deviatoric part, the bulk modulus (k) must be replaced by the shear modulus (μ) and superscript (s) by (d)). In this system, the elastic parts of the behavior laws are written in the adaptive incremental form presented in (Buffo-Lacarriere & Sellier 2009) in order to adapt to the mechanical behavior of concrete subjected to hydration.

$$\begin{cases} \dot{\tilde{\sigma}}_{(s)} = k^0 \dot{\varepsilon}^0_{(s)} + \left\langle \dot{k}^0 \right\rangle^- \varepsilon^0_{(s)} \\ \dot{\tilde{\sigma}}_{(s)} = k^{KV} \dot{\varepsilon}^{KV}_{(s)} + \left\langle \dot{k}^{KV} \right\rangle \varepsilon^{KV}_{(s)} + \dot{\eta}^{KV}_{(s)} \dot{\varepsilon}^{KV}_{(s)} + \eta^{KV}_{(s)} \ddot{\varepsilon}^{KV}_{(s)} \\ \dot{\tilde{\sigma}}_{(s)} = (\dot{\eta}^M_{(s)} \cdot Cc + \eta^M_{(s)} \cdot \dot{Cc}) \dot{\varepsilon}^M_{(s)} + (\eta^M_{(s)} \cdot Cc) \ddot{\varepsilon}^M_{(s)} \\ \dot{\varepsilon}_{(s)} = \dot{\varepsilon}^H_{(s)} + \dot{\varepsilon}^{KV}_{(s)} + \dot{\varepsilon}^M_{(s)} + \beta \cdot \dot{T} \end{cases} \quad (15)$$

where: - ε is the strain,
- T is the temperature,

- β is the thermal dilatation coefficient (parameter P^i) ($=10^{-5}$ °C^{-1}),

- Cc is the consolidation variable,

- k and μ are respectively the bulk and shear moduli(parameter P^i),

- η is the viscosity (parameter P^i).

- $\left\langle \dot{X} \right\rangle^{-} = \dot{X} < 0, 0$ otherwise.

The consolidation variable Cc expresses the fact that the viscosity is increased when the C-S-H layers come closer together during settling. As the progressive settling of the hydrates is limited by the compactness of the solid skeleton, the consolidation law is bounded using the material porosity. The consolidation variable is thus defined by Equation (16).

$$Cc = \frac{1-\varphi(-\Phi)}{\varphi(\varepsilon_M{}^{(s)}) - \varphi(-\Phi)}$$

$$\text{And} \quad \varphi(x) = \exp\left(\frac{x}{\varepsilon_M{}^{(s,d)k}}\right) \tag{16}$$

where: - φ is the consolidation function,

- Φ is the capillary porosity,

- $\varepsilon_M{}^{(s)}$ is the strain of the Maxwell module associated with the medium part of the stress,

- $\varepsilon_M{}^{k}$ is a characteristic strain that controls the consolidation speed.

4 NUMERICAL ADAPTATIONS FOR HARDENING CONCRETE

For an application to a hardening concrete, the damage model implementation needs particular updating of internal variables. In order to show the importance of this updating, an example is schematized in Figure 6 for a cracking state.

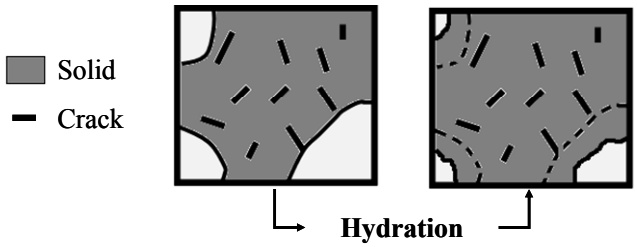

Figure 6. Possible mechanical damage evolution for hydration.

Let us assume cracking is modeled by a damage variable (D) defined as the averaged volume ratio (on the representative elementary volume REV) between voids due to cracks (Vc) and the solid (Vs).

As binder hydration produces undamaged hydrates, the crack volume is not modified by the hydration degree while the volume of solid increases proportionally to α. This physical observation can be modeled using Equation (17) which expresses the fact that the damage variable is defined in relation to mechanical properties themselves relative to the hydrated part of the REV.

$$\frac{\partial(\alpha \cdot D)}{\partial \alpha} = 0 \;\Rightarrow\; \frac{\partial D}{\partial \alpha} = -\frac{D}{\alpha} \tag{17}$$

Note that Equation (17) leads to a decrease in mechanical damage under the effect of hydration (which leads to self healing of the cement paste).

5 APPLICATION TO THE PREDICTION OF EARLY AGE CRACKING OF A MASSIVE STRUCTURE

The in situ structure chosen for this study was a massive experimental wall built by EDF on the construction site of the Civaux nuclear plant. The wall is 1.2 m wide, 1.9 m high and 20 m long and has a plane of symmetry at mid-length that justifies modeling only one half of the structure. The wall is reinforced by two wire grilles located at 5 cm from the lateral surface and contains spaces reserved for the prestressing cable guide tubes as presented in Figure 7.

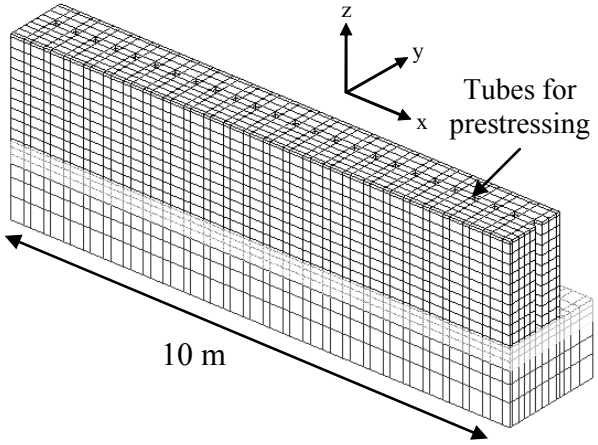

Figure 7. Mesh of the half structure.

First, the physicochemical model was applied to this structure cast with a composed binder (clinker + silica fume) to predict the variation of hydration degrees (see Figure 8) and of temperature. The temperature variations obtained at the core and near to the surface are presented in Figure 9. The model reproduces this temperature variation in the in situ structure. It can be seen that, because of its large dimensions, the structure undergoes a high increase in temperature, mainly in the core. The surfaces are subjected to thermal transfer by convection with the environment and have a lower temperature than the core.

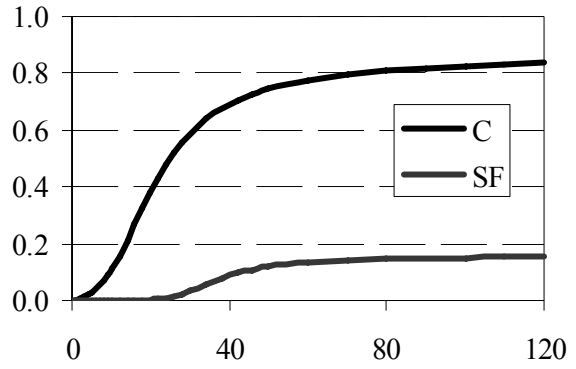

Figure 8. Variation of hydration degree of clinker (C) and silica fume (SF).

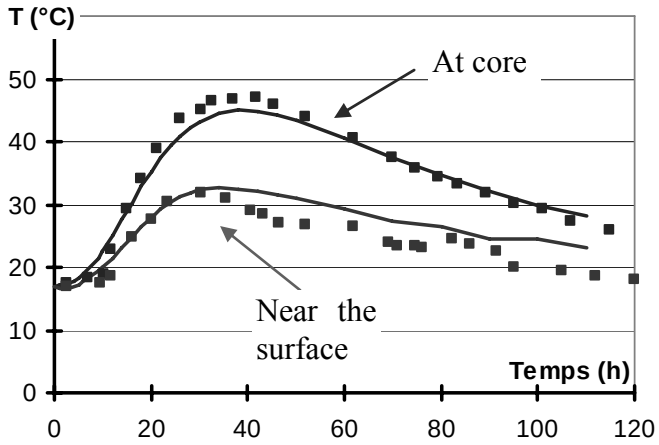

Figure 9. Variation of temperature in the core and near the surface (line: model; rectangles: experiments).

The mechanical model for hardening concrete was than applied using these physicochemical inputs (hydration degree and temperature variations). As we saw previously, the hydration degree (evaluated as a weighted average of the hydration degree of clinker and of silica fume) is used to calculate the variation of mechanical properties (Equation (14) with characteristics of totally hydrated concrete presented in Table 1).

Table 1. Parameters for mechanical characteristic variations.

Parameter	Value
k^0 (GPa)	27.2
$''^0$ (GPa)	16.7
k (GPa)	104.2
$''$ 'GPa)	38.9
$\eta^{(s)}$ (GPa.s)	$3.56.10^7$
$\eta^{(d)}$ (GPa.s)	$2.01.10^7$
$\eta^{(s)}$ (GPa.s)	$9.00.10^7$
$\eta^{(d)}_{k\infty}$ (GPa.s)	$1.75.10^9$
ε_{Λ} (m/m)	$2.8.10^{-5}$
Rc (MPa)	80.1
Rt_∞ (MPa)	4.13

The difference between surface and core temperatures generates a system of self balancing stresses with tension at the surface and compression at the core. On this structure, this leads to stresses too weak to produce superficial cracks just after the formwork removal.

The cracking observed on the structure 96 hours after casting (see Figure 10) was due to the global cooling of the wall that led to internal thermal contraction. As these strains were restrained by the raft foundation on the wall base, they gave rise to tensile stresses in the entire wall, with higher values at the core (where the temperature reached maximal values).

The crack was initiated near the prestressing cable guide tubes which constitute a weak point in the structure. Figure 10 highlights the good concordance between the model results and the observations made in situ.

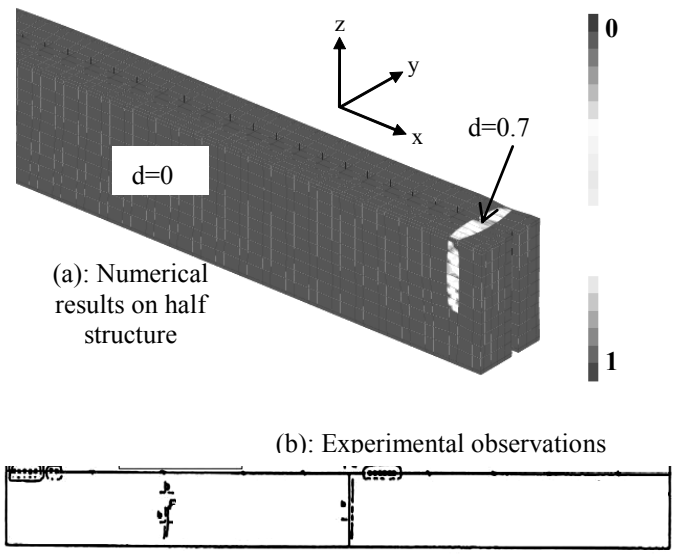

Figure 10. Longitudinal damage field (d_{xx}) 96 hours after casting.

In the proposed model, the crack opening can also be evaluated by the unsteadiness of the horizontal displacement of the node around the crack (see Figure 11). The values of crack opening for different distances to the surface are shown in Table 2. It can be noted that the crack opening is partially restrained by the wire grille and is maximal in the core.

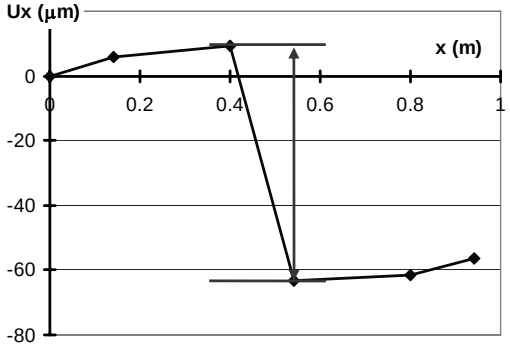

Figure 11. Crack opening calculation using the unsteadiness of the displacement.

Table 2. Crack opening.

Measurement location	Crack opening
At core (y=63 cm)	27.2
At y=35 cm	16.7
Near the steel (y=7 cm)	4.13

6 CONCLUSION

The paper presented a damage model based on a scalar variable in compression and on a fourth order tensor in tension so as to reproduce the unilateral and anisotropic behavior of concrete. In this work, the damage model is adapted to be applied on hardening concrete in order to take account of a self healing of the cement paste at early age. It was thus associated to a creep which is needed to a good evaluation of the stress developed at early age. The chemo-mechanical model thus proposed was finally successfully applied to the prediction of the early age cracking of a massive structure.

ACKNOWLEDGMENTS

The investigations and results reported herein are supported by the French national program CEOS.fr and the French National Research Agency (ANR) under the MEFISTO research program (control of cracking in concrete structures /grant VD08_323065).

The authors are also grateful to CEA for providing the finite element code Castem.

REFERENCES

Acker P., Ulm F-J. 2001. Creep and shrinkage of concrete: physical origins and practical measurements. *Nuclear Engineering and Design 203*: 143-158

Buffo-Lacarrière L. 2007. Prévision et évaluation de la fissuration précoce des ouvrages en béton. PhD. Thesis, Université de Toulouse.

Buffo-Lacarriere L., Sellier A. 2009. Numerical modelling of effects of chemical evolution on mechanical behaviour of concrete. In Alexender-Bertron, (ed.), *RILEM TC 211-PAE Final Conference. Concrete in Agressive Aqueous Environments*; *Toulouse, 3-5 June 2009*.

Buffo-Lacarrière L., Sellier A., Escadeillas G., Turatsinze A. 2007. Multiphasic finite element modeling of concrete hydration. *Cement and Concrete Research 37(2)*: 131-138.

Byfors, J. 1980. *Plain concrete at early ages*. PhD Thesis, Swedish, Cement and Concrete Institute, Sweden

De Schutter G. 2002. Finite element simulation of thermal cracking in massive hardening concrete elements using degree of hydration based material laws. *Computers and Structures 80*: 2035-2042

Hillerborg A., Modeer M., Petersson P. E. 1976. Analysis of crack formation and crack growth in concrete by means of fracture mechanics and finite elements. *Cement and Concrete Research 6*: 773-782.

Sellier A., Bary B. 2002. Coupled damage tensors and weakest link theory for the description of crack induced anisotropy in concrete. *Engineering Fracture Mechanics 69*: 1925-1939

Torrenti J-M., Bendoudjema F. 2005. Mechanical threshold of cementitious materials at early age. *Materials and Structures 38(277)*: 299-304.

Kachanov L.M. 1986. *Introduction to continuum damage mechanics.* Ed. Martinus Nijhoff, ISBN 90-247-3319-7, 135p

Benboudjema, F., Torrenti, J.M. 2008. Early age behaviour of concrete nuclear containments. *Nuclear Engineering & Design 238 (10)*: 2495-2506.